Physica ***D238****, 2009, No 14, 1203-1215.*

Coupled van der Pol – Duffing oscillators: phase dynamics and structure of synchronization tongues

A.P. Kuznetsov [1]*, N.V. Stankevich* [2]*, L.V. Turukina*[1]

[1] Kotel'nikov's Institute of Radio-Engineering and Electronics of RAS, Saratov Branch,
Zelyenaya, 38, Saratov, 410019, Russian Federation
[2] Saratov State University,
Astrakhanskaya, 83, Saratov, 410012, Russian Federation

Keywords: synchronization; coupled van der Pol oscillators; Adler's equation.

Abstract

Synchronization in the system of coupled non-identical non-isochronous Van fer Pol – Duffing oscillators with inertial and dissipative coupling is discussed. Generalized Adler's equation is obtained and investigated in the presence of all relevant factors affecting the synchronization (nonisochronism of the oscillators, their nonidentity, coupling of the dissipative and inertial type). Characteristic symmetries are revealed for the Adler's equation responsible for equivalence of some of the factors. Numerical study of the parameters space of the initial differential equations is carried out with a use of the method of charts of dynamic regimes in the parameter planes. Results obtained by both these approaches are compared and discussed.

Introduction

Systems of coupled self-oscillators are regarded as basic models in the theory of oscillators and nonlinear dynamics dealing with synchronization phenomenon and attendant effects. In general, this problem is characterized by a large number of parameters and by a complex bifurcation picture in the parameter space [1-13]. For the coupled systems one can observe many interesting oscillatory effects. Obviously, this problem is more complex than the problem concerning dynamics of one oscillator driven by an external periodic force [1,17].

Dynamics of coupled van der Pol oscillators and coupled van der Pol – Duffing oscillators is a subject of wide studies applicable in various areas of science and technology, relating, for example, to physical, chemical, biological and other systems. In this context, we have to mention, first of all, a fundamental monograph [1]; see also [2-16] and references therein. However, because of a relatively large number of parameters affecting dynamical phenomena in these systems, it is rather difficult to describe the general picture. Therefore, the studies usually are concentrated on certain fragments of the entire picture. For example, a case of a system of identical oscillators with dissipative coupling was analyzed in terms of the shortened, or amplitude equations [2]. A certain case of nonlinear coupling was studied in [10]. In paper [3] authors studied a system of identical and isochronous oscillators with combined (inertial and dissipative) coupling in terms of the generalized Adler's equation. As seen from the literature, identity of the oscillators is one of the commonly used traditional assumptions. A certain exception is the recent paper [13]. However, in this work nonisochronism of the oscillators was not taken into account. This lack seems essential; indeed, the nonisochronism has to be taking into account to write down a well-known normal form of Andronov – Hopf bifurcation for a single oscillator; so the isochronous system does not represent the generic case [1, 18]. Moreover, in accordance with [1], the nonisochronism provides one of mechanisms responsible for appearance of in-phase or out-phase synchronization. Thus, it seems necessary to generalize, systematize and interpret all the available results.

In the present work we intend to account in complex the following factors relevant for the dynamics of the coupled self-oscillators:

- dissipative coupling,

- inertial coupling,
- nonisochronism of the oscillators, i.e. a dependence of the rate of the phase variation on a radius of the oscillator orbit,
- nonidentity of the oscillators with respect to the parameters governing the Andronov – Hopf bifurcation and to the difference of the operating frequencies.

We shall consider the model of coupled van der Pol – Duffing oscillators within a framework of the following assumptions. First, we use the quasi-harmonic approximation. In addition, we assume that the perturbations of the orbits of the oscillators are weak in respect to the case of uncoupled subsystems. The latter allows us to pass to the phase equation, in the same way as in the classical theory of synchronization [1-3, 13]. The phase equation appears as a generalization of the known Adler equation [1]. As we shall demonstrate, to describe correctly effect of all the factors listed above it is necessary to take into account effects of the second order in the description of phase dynamics. (Exception is the dissipative coupling description of which may be based on accounting terms of the first order.) Therefore, the analysis requires a careful discussion. One more feature of the problem is a presence of number of symmetries associated with certain transformations of the phase variable. It implies equivalences of effect of some of the physical factors, as will be discussed in the course of the present work.

Description in terms of phase dynamics reflects physical nature and mechanisms of synchronization, but, certainly, not all the details of the general synchronization picture (like a complete set of regions of synchronization and their internal organization). Therefore, beside the discussion of the phase dynamics we will give illustrations for the dynamics of the initial differential equations. We use extensively a method of charts of dynamical regimes (see, e.g., [19, 20]). This method consists in numerical simulation of dynamics at a grid of pixels on some parameter plane supplied with analyses of nature of the dynamical regime coded by some color or gray tone. In this way, domains of different types of dynamical behavior are revealed on the parameters plane. This method is simple and productive from the point of view of the computer realization. With it, the whole set of synchronization tongues may be visualized automatically; as well, their internal organization can be resolved. On the other side, analytical results obtained for the phase dynamics arm us with a basic "strategy" for conducting the computations.

Part 1. Phase dynamics

1.1. Generalized phase dynamics equation

Let us consider a set of differential equations describing the coupled van der Pol – Duffing oscillators:

$$\begin{aligned} &\frac{d^2x}{dt^2}-(\lambda_1-x^2)\frac{dx}{dt}+(1-\frac{\Delta}{2})x+\beta x^3+\varepsilon(x-y)+\mu(\frac{dx}{dt}-\frac{dy}{dt})=0,\\ &\frac{d^2y}{dt^2}-(\lambda_1-y^2)\frac{dy}{dt}+(1+\frac{\Delta}{2})y+\beta y^3+\varepsilon(y-x)+\mu(\frac{dy}{dt}-\frac{dx}{dt})=0. \end{aligned} \qquad (1)$$

Here λ_1 and λ_2 are parameters responsible for the Andronov – Hopf bifurcation; Δ is the detuning parameter, proportional to a difference of the oscillator frequencies; β is parameter of the nonisochronism, that is dependence of the oscillation frequency on the amplitude; μ and ε are coupling parameters responsible for the dissipative and inertial coupling, respectively.[1].

First, let us turn to a quasi-harmonic approximation for the dynamics of the system (1). Let us assume that the solutions for dynamical variables x and y are represented as

$$x=\frac{1}{2}(ae^{it}+a^*e^{-it}),\ y=\frac{1}{2}(be^{it}+b^*e^{-it}), \qquad (2)$$

where $a(t)$ and $b(t)$ are complex amplitudes of the oscillators obeying the additional conditions standard for the method of slow amplitudes:

[1] Different authors use various terms for these types of coupling. In Ref. [3] both types are regarded as diffusion couplings. In Ref. [13] they are identified as dissipative and conservative ones. In Ref. [1] they are called the dissipative and the reactive couplings. In Ref. [2] they are identified as scalar and non-scalar couplings. Here we prefer to use the terms dissipative and inertial coupling [27]. The last term reflects both the “crossed” non-scalar type of the coupling (see [1]) and a specific action of the coupling on partial frequencies of the oscillators, even in absence of the dissipation.

$$\dot{a}e^{it} + \dot{a}^* e^{-it} = 0\,,\ \dot{b}e^{it} + \dot{b}^* e^{-it} = 0\,.$$

As follows, the expressions for the derivatives $\dot{x}$ and $\dot{y}$ are

$$\dot{x} = \frac{1}{2}(iae^{it} - ia^* e^{-it})\,,\ \dot{y} = \frac{1}{2}(ibe^{it} - ib^* e^{-it})\,. \tag{3}$$

Substitution of (2) and (3) into Eqs.(1), with multiplication by e^{-it} and subsequent time averaging leads to a set of truncated, or complex amplitude equations:

$$\begin{aligned}
\frac{da}{dt} &= \frac{\lambda_1 a}{2} - \frac{|a|^2 a}{8} + \frac{3i\beta|a|^2 a}{8} + \frac{i\varepsilon}{2}(a-b) - \frac{\mu}{2}(a-b) - \frac{i\Delta a}{4}, \\
\frac{db}{dt} &= \frac{\lambda_2 b}{2} - \frac{|b|^2 b}{8} + \frac{3i\beta|b|^2 b}{8} + \frac{i\varepsilon}{2}(b-a) - \frac{\mu}{2}(b-a) + \frac{i\Delta b}{4}.
\end{aligned} \tag{4}$$

With redefined variables and parameters: $\tau = t/2$, $z = a/2$, $w = b/2$, $\chi = 3\beta$, we rewrite these equations as

$$\begin{aligned}
\frac{dz}{d\tau} &= \lambda_1 z - |z|^2 z + i\chi|z|^2 z + i\varepsilon(z-w) + \mu(w-z) - \frac{i\Delta z}{2}, \\
\frac{dw}{d\tau} &= \lambda_2 w - |w|^2 w + i\chi|w|^2 w + i\varepsilon(w-z) + \mu(z-w) + \frac{i\Delta w}{2}.
\end{aligned} \tag{5}$$

Now, let us introduce real amplitudes and phases by means of the relations $z(t) = R(t)\exp(i\varphi_1)$ and $w(t) = r(t)\exp(i\varphi_2)$. Separating real and imaginary parts, from Eqs.(5) we arrive at the following set of equations for the real amplitudes *R, r* and phases φ_1 and φ_2:

$$\begin{aligned}
\frac{dR}{d\tau} &= R(\lambda_1 - \mu) - R^3 + \mu r\cos(\varphi_2 - \varphi_1) + \varepsilon r\sin(\varphi_2 - \varphi_1), \\
\frac{dr}{d\tau} &= r(\lambda_2 - \mu) - r^3 + \mu R\cos(\varphi_1 - \varphi_2) + \varepsilon R\sin(\varphi_1 - \varphi_2), \\
\frac{d\varphi_1}{d\tau} &= \chi R^2 + \varepsilon - \frac{r}{R}\varepsilon\cos(\varphi_2 - \varphi_1) + \frac{r}{R}\mu\sin(\varphi_2 - \varphi_1) - \frac{\Delta}{2}, \\
\frac{d\varphi_2}{d\tau} &= \chi r^2 + \varepsilon - \frac{R}{r}\varepsilon\cos(\varphi_1 - \varphi_2) + \frac{R}{r}\mu\sin(\varphi_1 - \varphi_2) + \frac{\Delta}{2}.
\end{aligned} \tag{6}$$

Subtracting the equation for φ_1 from the equation for φ_2 and designating, we obtain the equations

$$\begin{aligned}
\frac{dR}{d\tau} &= R(\lambda_1 - \mu) - R^3 + \mu r\cos\varphi + \varepsilon r\sin\varphi, \\
\frac{dr}{d\tau} &= r(\lambda_2 - \mu) - r^3 + \mu R\cos\varphi - \varepsilon R\sin\varphi, \\
\frac{d\varphi}{d\tau} &= \Delta + \chi(r^2 - R^2) + \varepsilon\left(\frac{r}{R} - \frac{R}{r}\right)\cos\varphi - \mu\left(\frac{r}{R} + \frac{R}{r}\right)\sin\varphi,
\end{aligned} \tag{7}$$

where $\varphi = \varphi_2 - \varphi_1$. Here one of the parameters (λ_1 or λ_2) may be eliminated by renormalization. It is convenient to set $\lambda_1 = 1 + \delta$ and $\lambda_2 = 1 - \delta$, where δ is the parameter of nonidentity. Then, a final form of the truncated equations [13] reads:

$$\begin{aligned}
\frac{dR}{d\tau} &= R(1 + \delta - \mu) - R^3 + \mu r\cos\varphi + \varepsilon r\sin\varphi, \\
\frac{dr}{d\tau} &= r(1 - \delta - \mu) - r^3 + \mu R\cos\varphi - \varepsilon R\sin\varphi, \\
\frac{d\varphi}{d\tau} &= \Delta + \chi(r^2 - R^2) + \varepsilon\left(\frac{r}{R} - \frac{R}{r}\right)\cos\varphi - \mu\left(\frac{r}{R} + \frac{R}{r}\right)\sin\varphi.
\end{aligned} \tag{8}$$

Now let us derive a phase equation using assumption that the nonidentity, the nonisochronism and the couplings are weak.

To start, consider equations for the real amplitudes of unperturbed uncoupled oscillators

$$\frac{dR}{d\tau} = R - R^3, \frac{dr}{d\tau} = r - r^3$$

and remark that they have a stable stationary solution corresponding to identical orbits of radius $R = r = 1$. For the perturbed solutions we set $R = 1 + \widetilde{R}$ and $r = 1 + \widetilde{r}$. The tilde marks the perturbation terms. Substituting these expressions in (8) and ignoring terms of the higher order, we obtain

$$\begin{aligned} \frac{d\widetilde{R}}{d\tau} &= -2\widetilde{R} + \mu(\cos\varphi - 1) + \varepsilon\sin\varphi + \delta, \\ \frac{d\widetilde{r}}{d\tau} &= -2\widetilde{r} + \mu(\cos\varphi - 1) - \varepsilon\sin\varphi - \delta. \end{aligned} \tag{9}$$

Because of strong dumping for the deflections of the amplitudes [1], their values approach rapidly the perturbed stationary solution. Using this fact, we estimate easily the perturbations as

$$\widetilde{R} = \frac{1}{2}[\mu(\cos\varphi - 1) + \varepsilon\sin\varphi + \delta],\ \widetilde{r} = \frac{1}{2}[\mu(\cos\varphi - 1) - \varepsilon\sin\varphi - \delta]. \tag{10}$$

As follows from (10), the dissipative coupling tends to make orbits of both oscillators closer. In turn, the inertial coupling may cause growth of difference of the states of the oscillators. For example, at $\varphi \cong \pi/2$ and $\varepsilon > 0$ the coupling stimulates growth of the orbit radius for the first oscillator and decrease of that for the second one. This remark is important for subsequent discussion of difference in behavior of the systems with different types of coupling.

Substituting $R = 1 + \widetilde{R}$ and $r = 1 + \widetilde{r}$ in the third equation of the set (8), we get

$$\frac{d\varphi}{d\tau} = \Delta + 2\chi(\widetilde{r} - \widetilde{R}) - 2\mu\sin\varphi + 2\varepsilon(\widetilde{r} - \widetilde{R})\cos\varphi. \tag{11}$$

Now we are ready to write down a generalized Adler's equation for system (1) accounting all the factors we consider. Substituting (10) in (11), after some transformations we obtain the desired phase equation [2]

$$\frac{d\varphi}{d\tau} = \Delta - 2\chi\delta - 2(\mu + \chi\varepsilon)\sin\varphi - \varepsilon^2\sin 2\varphi - 2\varepsilon\delta\cos\varphi. \tag{12}$$

It is convenient to rewrite the equation via an effective potential as

$$\frac{d\varphi}{d\tau} = -\frac{\partial U(\varphi)}{\partial\varphi}, \tag{13}$$

where

$$U(\varphi) = -(\Delta - 2\chi\delta)\varphi - 2(\mu + \chi\varepsilon)\cos\varphi - \frac{1}{2}\varepsilon^2\cos 2\varphi + 2\varepsilon\delta\sin\varphi. \tag{14}$$

Obviously, the minima of the potential $U(\varphi)$ give rise to stable synchronous regimes of oscillations, while the maxima correspond to unstable synchronous states of the system of coupled oscillators.

1.2. Effect of different factors on phase dynamics

Now let us discuss the effect of each factor (couplings, nonisochronism, and nonidentity) on the phase dynamics.

[2] Comparing the equations (12), (8) and similar equations from [1, 3, 13], it should be noted that different authors use different choices for signs of the parameters and for the oscillators phases. E.g., in [1] the authors use opposite sings for nonisochronism χ and inertial coupling ε, and in [13] the authors use a different normalization for the control parameter obtaining the ralations analogous to our equations (8).

Dissipative coupling. The term in the effective potential associated with the dissipative coupling is

$$U(\varphi) = -2\mu\cos\varphi + \ldots \quad (15)$$

In isochronous case it has a minimum at $\varphi = 0$. Thus, the dissipative coupling tends to synchronize the oscillators "in-phase", while the case $\varphi = \pi$ corresponds to an unstable state.

Inertial coupling. The corresponding term in the effective potential is

$$U(\varphi) = -\frac{1}{2}\varepsilon^2\cos 2\varphi + \ldots \quad (16)$$

As follows from this expression, the inertial coupling reveals itself in the second order synchronization effects. Further, we shall see that the synchronization tongue in a plane of coupling parameter and frequency detuning parameter has a very narrow cusp at small coupling. Another feature of the case of the inertial coupling is intrinsic phase bistability. Indeed, the potential (16) gives rise to two stable states, $\varphi = 0$ and $\varphi = \pi$. Thus, the inertial coupling can synchronize the oscillators either in-phase, or out-of-phase, depending on initial conditions. Two unstable states are placed between the stable states, and, hence, the potential (16) has four stationary states.

Nonisochronism. This factor, in the presence of inertial coupling, produces an addend correction to the dissipative coupling term in the potential:

$$U(\varphi) = -2(\mu + \chi\varepsilon)\cos\varphi + \ldots \quad (17)$$

Thus, the effect is of the second order too. It is due to the combination of the nonisichronism and the inertial coupling. The corresponding mechanism is described in [1] and may be explained as follows. Let the phase of the second oscillator is greater than phase of the first oscillator by $\pi/2$. According to (10), the orbit of the second oscillator will have a smaller radius than that of the first oscillator. Then, as seen from the phase equation (6), due to the nonisochronism, the angular velocity of the first oscillator will increase, and the angular velocity of the second oscillator will decrease. It means that the oscillators will become closer in the angular coordinate. Thus, in accordance with (17), the nonisichronism combined with inertial coupling produces the same effect as the dissipative coupling. However, in the case of a negative parameter of the nonisochronism χ, the situation is inverse: the angular velocity of the first oscillator will decrease, while that of the second oscillator will increase. As a result, the oscillators will go away, out-of-phase. It represents an example of the out-of-phase synchronization. As seen from (17), this situation is similar to the case of negative value of μ. Thus, for the sake of generality, it is necessary to consider both $\mu>0$ and $\mu<0$. The latter may be named ***the active coupling***[3]. In the case of such coupling, the out-of-phase stable synchronization regimes should be expected.

Nonidentity. In a system with inertial coupling, a small nonidentity effects in the second order too. The corresponding term in effective potential is

$$U(\varphi) = 2\varepsilon\delta\sin\varphi + \ldots \quad (18)$$

With this potential the synchronization takes place at the phase shift $3\pi/2$ and $\pi/2$, the stability of these states is determined by a sign of the product $\varepsilon\delta$.

In a nonisochronous system, the nonidentity also results is a small addition to the frequency detuning, since the corresponding term in the effective potential is

$$U(\varphi) = -(\Delta - 2\chi\delta)\varphi + \ldots \quad (19)$$

We conclude that there are several mechanisms, which lead to synchronization with various phase differences, namely, 0, $\pi/2$, π, $3\pi/2$. Besides, the phase multistability is possible in a system with inertial coupling. In the next sections we discuss these various cases in more details.

[3] The concept of active coupling seems natural from the formal point of view. In electronics, a resistor may provide dissipative coupling in coupled van der Pol oscillators in practical design. To arrange the active coupling it is necessary to create a "negative resistance", for example, with a use of an operational amplifier. This is not so difficult; so, ignoring a possibility of negative values for the dissipative coupling terms seems rather a historical tradition.

Part 2. Dissipatively-coupled oscillators

2.1. Dissipative coupling. Phase equation

For a system with purely dissipative coupling the phase equation reads

$$\frac{d\varphi}{d\tau} = \Delta - 2\mu\sin\varphi . \qquad (20)$$

It is the classical Adler equation [1]. As seen from (20), the equilibrium points can be determined from the relation

$$\frac{\Delta}{2\mu} = \sin\varphi . \qquad (21)$$

Let us consider a diagram on the parameter plane of the frequency detuning and coupling coefficient (Δ, μ) shown in Fig.1, where the half-plane $\mu > 0$ is presented. Real solutions of the equation (21) exist inside of a synchronization tongue bounded by the lines $\mu = \pm\Delta/2$. A stable state in this tongue corresponds to "in-phase" synchronization. At $\Delta = 0$ in the stationary state the phase difference φ is precisely equal to zero.

The picture for the active coupling, $\mu < 0$, is symmetrical with respect to Δ axis, and instead of the "in-phase" mode the "out-of-phase" mode takes place in the stable stationary synchronous state.

According to (12), a small nonidentity in the control parameters δ does not affect the form of synchronization region for the system with purely dissipative coupling. The same is valid for small nonisichronism χ, since the dissipative coupling effects identically on orbits of both oscillators, and the frequencies of their oscillations remain equal. However, if we introduce both nonidentity and nonisochronism, then, as follows from (12), we obtain a constant addition to the frequency detuning in the phase equation. It means that synchronization region is shifted to the right or to the left, depending on the sign of the addition. However for initial differential equations (1) the action of these two factors appears to be much more essential.

2.2. Numerical study of the coupled oscillators. General remarks

Now let us turn to results of numerical studies of the initial differential equations of coupled van der Pol – Duffing oscillators (1).

The phase equation (12) contains five parameters that affect the phase dynamics and synchronization picture. However, for the system (1) the number of relevant parameters is even greater, since along with the nonidentity parameter $\delta = \frac{\lambda_1 - \lambda_2}{2}$ the dynamics depends on the values of parameters λ_1 and λ_2 themselves. In the strict sense, the quasi-harmonic approximation is correct only in a case of small λ_1 and λ_2. We shall choose these parameters as $\lambda_1, \lambda_2 \approx 1$. On one hand, this choice allows us to reveal features of the phase dynamics, at last at a qualitative level. On the other hand, it allows illustrating the complex dynamical phenomena for the initial equations of coupled oscillators, the dynamics of which is far richer.

To illustrate visually the synchronization picture, we will use the charts of dynamical regimes [19, 20]. The method is based on numerical simulation of dynamics at a grid of pixels on some parameter plane supplied with analyses of a type of the dynamical regime; if the periodicity is detected, the pixel is marked then by a certain gray tone depending on the period. Regions of periodic behavior will be shown in white and gray tones. The black color will represent chaos and quasi-periodical regimes. The periods of cycles are specified with a use of the method of Poincaré sections. The period is determined as number of points of intersection of the phase trajectory on the attractor with a hyper-surface in the phase space $\dot{y} = 0$ chosen to construct the return map. Only those crossings are accounted that correspond to direction of crossing of the surface from one side. Domains of different periodic regimes are shaded with different gradations of grey.

Before the discussion of the illustrations we have to make a remark. In computations, it is easy to choose any sign of the parameters. It is not so for real systems: a change of sign of coupling may require using another radio-engineering element, say a device involving operation amplifier instead of a simple

resistor. Nevertheless, to get entire picture of dynamical phenomena, it is useful to consider different variants of selection of signs; so, we do not restrict it in the computer experiments.

2.3. Numerical results for the dissipatively coupled oscillators

Let us consider a chart of dynamical regimes for dissipatively coupled identical van der Pol oscillators shown in Fig.2. [4] Here we take $\lambda_1 = \lambda_2 = 1$. If $|\Delta| > 2$, the orbit goes to infinity[5]. In Fig. 2 one can see symmetric synchronization region bounded by the lines $\mu = \pm\frac{\Delta}{2}$ in agreement with the expression (21). Synchronization regions for the cases of dissipative and active coupling are visually identical, as predicted by analysis of the phase dynamics.

Two projections of the attractor in the four-dimensional phase space of system (1) are shown in Fig.3. One is the phase portrait of the first oscillator in the $(x,\dot{x})$ plane, and another is a projection on the plane (x,y). We consider here a case of very small frequency detuning in presence of dissipative or active coupling. From Fig.3 it follows, that in the case of dissipative coupling the oscillators are synchronized "in-phase" ($\varphi = 0$). In the case of active coupling they synchronize "out-of-phase" ($\varphi = \pi$). Moreover, according to (10), the radius of the oscillators orbits decreases with the dissipative coupling and increases with the active coupling. In the last case, the limit cycle is deformed just like it was for the uncoupled systems under increase of λ [17]. On the parameters plane presented in Fig.2, one can see a set of higher order synchronization regions too. The regions corresponding to the frequencies ratio 3:1 (and 1:3) are the most significant. These regions are not described by the equations (7).

Fragments of the chart presented in Fig.2 are shown magnified in Fig.4. From these charts we conclude that the dissipative and active couplings are not equivalent, if we consider the whole organization of the synchronization domains. It makes an essential difference in comparison with the phase dynamics. Really, for the active coupling the synchronization regions are wider and are characterized by more complex internal organization. The explanation is that according to (10), dissipative coupling diminishes the "effective" value of the parameter λ, while the active coupling would increase it. Thus, in a system with active coupling, the oscillations correspond to greater values of the control parameter.

2.4. Dissipative coupling, nonidentity and nonisochronism

Now let us add the factors of nonidentity and nonisochronism in a system with dissipative coupling. From the phase equation (12) it follows that in the absence of the inertial coupling these factors do not affect the synchronization picture. We will consider the case when the control parameter λ is not small.

First, let us have nonidentity without nonisochronism. Let $\lambda_1 = 2,\ \lambda_2 = 1$ (i.e. $\delta = 0{,}5$). The chart of dynamical regimes on the plane (Δ, μ) for this case is shown in Fig. 5. One can see that the synchronization region is symmetric at small Δ, as predicted with the phase equation. But it becomes asymmetric at larger Δ: the synchronization threshold is essentially lower at negative Δ, than that at positive ones. This observation can not be explained within the framework of the phase equation (12)[6].

Now, let us add nonisochronism in the system with dissipative coupling (Fig. 6)[7]. In this case, the tip of the synchronization region is located at Δ=0, and it is strictly symmetric. However, we observe that the set of synchronization regions of higher order transforms essentially. Now, the synchronization regions appear to have complex internal organization, which is similar to that for a classical circle map

---

[4] Because of the concrete choice of the Poincaré section in our computations, only one set of synchronization tongues (from one side of the main synchronization region) is visible on the chart in the course of the computations based on the used procedure; the second set remains unresolved (indicated as a region of period 1). Accounting symmetry of the system in respect to exchange of the oscillators, we, nevertheless, paint these tongues with the same colors as those relating to the first set.

[5] Note, that the "oscillator death" region occurring often in the systems with dissipative coupling, is not observed in the model (1) at $\lambda_1 = \lambda_2 = 1$ [1,2]. It appears at smaller values of the parameters λ_1 and λ_2.

[6] Here we present the case, in which the "oscillator death" effect is absent. In its presence, the nonidentity is more important; the details are discussed e.g. in [25,26].

[7] Parameter β (or χ=3β in the truncated equations) is a parameter of nonisochronism, and we always use the term nonisochronous exclusively meaning the situations of non-zero β. To be precise, the oscillations in the system (1) with large amplitude are nonisochronous even at β=0; that is not accounted in the terminology we accept here.

[1]. One can see the characteristic structures ("crossroad area") [21,22] in the fragment of the picture presented in Fig. 6b; it is a typical composition of curves of tangent (saddle-node) bifurcations and period doubling bifurcations. The boundary of the main synchronization region colored in white is a line of saddle-node bifurcation (Fig.6b). Synchronization regions of higher order are stretched along this line.

It should be noted, that the system (1) with the nonlinearity term βx^3 can demonstrate regimes, which have no analogues within the framework of the truncated equations. Really, it is possible to write the potential

$$U(x)=\frac{1}{2}(1-\frac{\Delta}{2})x^2+\frac{1}{4}\beta x^4,\ U(y)=\frac{1}{2}(1-\frac{\Delta}{2})y^2+\frac{1}{4}\beta y^4 \qquad (22)$$

for uncoupled oscillators. If $\Delta>2$, or $\Delta<-2$, then, one of the oscillators has a maximum of potential instead of minimum at the origin. Then, at $\beta>0$ the oscillators are characterized by "two-well" potentials. Hence, there are no oscillations with some certain frequency near the origin. Thus, we can not use the method of slow amplitudes to obtain truncated Eqs. (7). Nevertheless, the equations of the system (1) can be solved numerically in this case too. As follows from (22), there is no regions in the parameters plane, in which the trajectories would go to infinity at small β. Then, the range of frequency detuning Δ can be increased (compare Fig. 2 and Fig. 6a).

In Fig. 7 a fragment of the chart of dynamical regime is presented in a vicinity of the point $\Delta=2$. It corresponds to transition from the one-well to the two-well potential in the first oscillator. In this figure, the border of synchronization region is of more complex organization at $\Delta>2$ in comparison with that we see earlier. To make it clear, in Fig. 7b the bifurcation curves are shown obtained numerically. One can see a line of saddle-node bifurcation and two lines of Neimark-Sacker bifurcation. One of them has a terminal point on a line of the saddle-node bifurcation. This is a point of resonance 1:1. The terminal point of the second line is a point of resonance 1:2. This point is located on a line of period-doubling bifurcation. There is also some special point of tangency of two lines of Neimark-Sacker bifurcations. In the right half of Fig. 7a, one can observe also the period-doubling bifurcation cascade as parameter of coupling is decreased.

Now let us add both nonidentity and nonisochronism in the system with dissipative coupling (Fig. 8a). In this case, the main synchronization region is strongly displaced towards the domain of positive detuning Δ>0. From the phase equation (12), we obtain an approximate estimate $\Delta=2\chi\delta=6\beta\delta\approx 3$. Displacement is so big, that the tip of the synchronization region appears outside of the area $-2<\Delta<2$. So, here we have a strong asymmetry of the synchronization picture in comparison with that in the isochronous case.

Fig. 8b shows a magnified fragment of synchronization regions from the panel (a). In Fig. 8c we present in the same scale main bifurcation curves and points found numerically. One can see that the saddle-node bifurcation curve has a cusp point, and curves of saddle-node and Neimark-Saker bifurcations have the common point (a codimension 2 bifurcation point, resonance 1:1). This configuration is typical for synchronization problems, e.g. it is observed in the van der Pol system under periodic forcing [17].

In Fig. 8b one can see a set of islands of period-doubled regimes inside the synchronization regions. Observe that the synchronization domains are overlapping. Synchronization regions are stretched along a line of the Neimark-Sacker bifurcation *NS* (compare with the alternative case of the saddle-node bifurcation line in Fig.6b). In the right half of Fig. 8b, the line of saddle-node bifurcation appears as an edge of the main synchronization region. Near the point $\Delta=-0.2$ one can see the transition from the line of saddle-node bifurcation to the Neimark-Saker bifurcation curve.

Part 3. Inertial-coupled oscillators

3.1. Inertial coupling

Now let us turn to the case of oscillators with inertial coupling. For identical isochronous oscillators we have

$$\frac{d\varphi}{d\tau}=\Delta-\varepsilon^2\sin 2\varphi, \qquad (23)$$

and the boundaries of the synchronization region are expressed by the relation

$$\Delta = \pm\varepsilon^2 . \qquad (24)$$

Thus, the synchronization region has a very narrow tip (Fig. 9) (a square root singularity) since the synchronization is a "second order" effect in this case, as pointed out earlier. However, the synchronization region extends quickly as ε grows. (In Fig. 9 we present only the top half-plane, ε>0; note that in fact the picture is symmetric with respect to inversion of the sign of ε.)

The phase bistability inside the synchronization region (shown in gray) is an essential feature of dynamics for this type of coupling. Two coexisting states arise or disappear simultaneously, just at the passage across the boundary of the synchronization region. The bifurcation diagram obtained along the arrow line indicated in Fig. 9a is shown in panel (b).

Now let us turn to discussion of charts of dynamical regimes for the system (1) with inertial coupling. In Fig. 10a the chart is shown for identical isochronous oscillators with $\lambda_1 = \lambda_2 = 1$. First of all, we note that the main synchronization region (white) has an extremely narrow tip (the square root singularity), in accordance with the analysis of the phase equation (23). In Fig. 10b we present a fragment from Fig. 10a showing magnification of the tip of the synchronization region. Observe violation of symmetry predicted by the analysis of the phase equation: the disposition of the synchronization tongues looks surely different at ε>0 and at ε<0.

The region of divergence of the trajectories go to infinity appears because the inertial coupling changes frequencies of the oscillations in the subsystems. Indeed, in this case the isochronous system (1) can be characterized by potential

$$U(x,y) = \frac{1}{2}\left[(1 - \frac{\Delta}{2} + \varepsilon)x^2 - 2\varepsilon xy + (1 + \frac{\Delta}{2} + \varepsilon)y^2 \right]. \qquad (25)$$

The potential has a local minimum only if

$$\varepsilon > \frac{1}{2}\left(\frac{\Delta^2}{4} - 1 \right). \qquad (26)$$

Otherwise, the critical point becomes a saddle, and in this case divergence of the trajectories to infinity can be observed. The boundary of this region is given by

$$\varepsilon = \frac{1}{2}\left(\frac{\Delta^2}{4} - 1 \right) \qquad (27)$$

Looks like a parabola and may be seen in Fig. 10. A threshold value for coupling, at which the oscillations are still possible, is $\varepsilon = -1/2$.

3.2. Inertial coupling and nonidentity

Now let us consider non-identical subsystems with inertial coupling. In this case the phase equation became

$$\frac{d\varphi}{d\tau} = \Delta - \varepsilon^2 \sin 2\varphi - 2\varepsilon\delta\cos\varphi . \qquad (28)$$

From this, the equation for the phase equilibrium states follows:

$$\Delta = \varepsilon^2 \sin 2\varphi + 2\varepsilon\delta\cos\varphi . \qquad (29)$$

If ε is very small, the first term in (29) may be ignored. Then, the synchronization region will have a traditional "corner" form ($\varepsilon = \pm\Delta/2\delta$), instead of the square root cusp singularity. Thus, the synchronization region becomes wider as δ is increased.

The case of $\Delta = 0$ can be treated analytically. From (29) we se that one of two conditions must be valid at an equilibrium point:

$$\begin{aligned} &\cos\varphi = 0, \\ &\varepsilon\sin\varphi + \delta = 0. \end{aligned} \qquad (30)$$

At small ε, as follows from the first equality, there are two equilibriums: $\varphi = \pi/2$ and $\varphi = 3\pi/2$, which do not depend on the coupling strength. The first one is unstable, and the second is stable. Two more equilibrium points appear at a threshold value $\varepsilon = \delta$, for which second relation (30) is valid. They arise at a phase $\varphi = 3\pi/2$ and tend to $\varphi = \pi$ and $\varphi = 2\pi$ as ε grows. The bifurcation diagram for this case is shown in Fig. 11b demonstrating a pitchfork bifurcation at $\varepsilon = \delta$. Hence, bistability arises at $\varepsilon > \delta$. It may be said that the nonidentity destroys the common boundary of synchronization for the bistable states; after the transition it appears to be different for each of them.

Let us evaluate the boundaries of the synchronization region. The corresponding lines on the parameter plane are the curves of saddle-node bifurcation. We get them by differentiating expression (29) with respect to φ. Then,

$$0 = \varepsilon\cos 2\varphi - \delta\sin\varphi. \qquad (31)$$

From this, we obtain the boundaries of the synchronization region on the plane (Δ, ε) in parametric form

$$\Delta = \varepsilon^2\sin 2\varphi + 2\varepsilon\delta\cos\varphi, \quad \varepsilon = \frac{\delta\sin\varphi}{\cos 2\varphi}. \qquad (32)$$

The case under consideration is characterized by three parameters Δ, ε and δ. Figure 11a shows disposition of the synchronization region in the cross-section of the parameter space with the plane (Δ, ε) at fixed δ=0.5. Observe that the saddle-node bifurcations lines for different equilibrium points do not coincide. The cusp point is located at $(0, \delta)$ on the parameter plane, and the saddle-node bifurcations lines merge at this point. The panel (b) presents the bifurcation diagram along the line of Δ=0. Figure 12 shows the chart on (Δ, δ) parameters plane at fixed ε=0.5 (a) and the bifurcation diagram drawn along the line of Δ=0. Here again one can see a cusp point on the chart, but its tip is directed upwards; so, the region of bistability is located in the bottom part of the picture. So, there are two possible types of disposition of the synchronization regions[8].

We have discussed a case of δ>0. In this case the control parameter of the first oscillator is larger than the control parameter of the second oscillator. From (28) it follows that inversion of the sign of δ is equivalent to simultaneous inversion of signs of phase φ and the frequency detuning Δ.

In Fig. 13 we present a chart of dynamical regimes for the system (1) in the case of nonidentical subsystems with inertial coupling on the parameter plane (ε, Δ). In the central part of the chart there is a region of bistability, which may be thought as represented by overlapping "sheets" of the chart. Two "sheets" correspond to two attractors arising from different initial conditions, but corresponding to regimes of the same period; so, the overlapping should not be visualized. However, the saddle-node bifurcation takes place at the edges of the "sheets", and there the convergence to the attractors becomes very slow, so, the computer program fails to estimate the period. As a result, the bifurcation lines appear visible [19,20], as seen in Fig. 13. Nevertheless, it is necessary to use accurate bifurcation analysis for more detailed description.

Figure 14 shows a chart of dynamical regimes for the system (1) in the case of nonidentical subsystems with inertial coupling in the parameter plane (δ, Δ). This is the second type of structure of a synchronization region. In this case, the synchronization region leans on a final interval of frequency detuning Δ axis. This result agrees with the prediction of the phase dynamics analysis. One can see two "sheets" forming the region of bistability. There is a correspondence between this picture and Fig. 12.

3.3. Phase equation symmetries

The phase equation (12) possesses certain symmetries, which result in equivalence of some physical

[8] Existence of two types of synchronization regions was noted in the article [3]. However, in that work, only the case of isochronous system with dissipative and inertial coupling was investigated (see also section 2.3 of the present paper).

factors affecting the synchronization phenomena. Here we shall discuss this in more details.

In the previous section, we added nonidentity to a system with inertial coupling. Now let us add nonisochronism instead of the nonidentity to the same system with inertial coupling. Then, from expression (12) we obtain:

$$\frac{d\varphi}{d\tau} = \Delta - 2\chi\varepsilon\sin\varphi - \varepsilon^2\sin 2\varphi . \qquad (33)$$

A variable change $\varphi = \pi/2 - \theta$ in this relation yields

$$-\frac{d\theta}{d\tau} = \Delta - \varepsilon^2\sin 2\theta - 2\chi\varepsilon\cos\theta . \qquad (34)$$

The formula (34) coincides with (28), except for a sign of the derivative, if we take $\chi=\delta$. (Note that (28) is a phase equation for nonidentical oscillators with inertial coupling.) Thus, presence of nonidentity or nonisochronism gives rise to appearance of the bifurcation diagrams are equivalent up to the phase shift by $\pi/2$ and inverse stability type of the equilibrium points. Hence, the arrangement of the bifurcation lines will be identical in both cases.

The same features are intrinsic to identical isochronous oscillators with dissipative and inertial couplings. In this case, we have the phase equation:

$$\frac{d\varphi}{d\tau} = \Delta - 2\mu\sin\varphi - \varepsilon^2\sin 2\varphi . \qquad (35)$$

At fixed $\varepsilon=1$ the relation (35) coincide with (33), if we set $\mu = \chi$. Thus, the synchronization regions for a nonisochronous system in the plane (Δ, χ) and those for a system with dissipative and active coupling in the plane (Δ, μ), are congruent.

Note, that the synchronization pictures will be similar at other values of ε too. However, in those cases it is necessary to rescale the parameter value according to a certain rule. Indeed, let us redefine parameters as

$$\Delta \to \varepsilon^2\Delta ,\ \varepsilon \to \varepsilon^2 ,\ \chi \to \mu ,$$

Then, the formula will coincide with (35), except the scale of time variable that has to be renormalized by factor ε^2. Thus the synchronization pictures will be equivalent, if we recalculate the inertial coupling strength by means of the $\varepsilon \to \varepsilon^2$.

We conclude that nonidentity, nonisochronism and dissipative coupling in a system with inertial coupling being added individually give rise to the same organization of the parameter space. Thus, the pictures in Fig. 13 and Fid. 14a are of the standard type for the synchronization regions.

In Fig. 14 we compare charts of dynamical regimes drawn for the system with nonidentity and inertial coupling (Fig. 14a) and for the system with dissipative and inertial couplings (Fig. 14b). One can see a remarkable correspondence of both figures. It concerns not only the form of the main synchronization region, but, to some extent, the whole structure of disposition of the synchronization regions of higher order.

3.4. Inertial coupling, nonidentity and nonisochronism

All the cases we discussed were characterized by two relevant parameters. Now, let us turn to a more general situation and consider a three essential parameter family. Herewith equivalence between different physical factors will be disturbed, since the solutions corresponding, for example, to a shift of the phase by $\pi/2$ are no equivalent longer.

For nonidentical, nonisochronous subsystems with inertial coupling we have the following equation

$$\Delta = 2\chi\delta + 2\chi\varepsilon\sin\varphi + \varepsilon^2\sin 2\varphi + 2\varepsilon\delta\cos\varphi . \qquad (36)$$

Boundaries of synchronization regions are given by the relation

$$\chi\cos\varphi + \varepsilon\cos 2\varphi - \delta\sin\varphi = 0 \qquad (37)$$

that yields

$$\delta = \frac{\varepsilon \cos 2\varphi + \chi \cos \varphi}{\sin \varphi}. \qquad (38)$$

Let us study transformations of synchronization region on the plane (Δ, δ) using (36) and (38), as χ is varied. The corresponding structures are shown in Fig. 15. Now, in contrast to Fig. 12, we draw the domains both for positive and negative δ. It is of relevance from the point of view of the transformations we observe.

One can see that synchronization region becomes asymmetric as χ grows (Fig. 15b). Two fold-bifurcation curves come closer and merge at $\chi = 0{,}5$ (Fig. 15c), and two new cusps appear at the origin, later they are branching off (Fig. 15d). The corresponding transformation is called "a horn to a horn" [23, 24.] (See in this context Fig. 15c.) The threshold parameter value may be found analytically if we suppose that two points of intersection of the fold lines with Δ axis merge and disappear at $\delta = 0$ (the transition from Fig. 15b to Fig. 15d). Therefore, setting $\delta = 0$ in (38) we obtain

$$\varepsilon \cos 2\varphi = -\chi \cos \varphi. \qquad (39)$$

Real roots of the equation (39) merge and disappear at $\cos\varphi = \pm 1$ and there we have $\chi = \pm\varepsilon$, which corresponds to Fig. 15c.

Further, the pairs of "new" and "old" cusps form the typical structures called "dovetail" configurations [23,24] (Fig. `15d, e). The cusp points constituting them, in turn, merge and disappear (Fig. 15e, f). The corresponding co-dimension 3 bifurcation point obeys the set of equations

$$\chi \cos\varphi + \varepsilon \cos 2\varphi - \delta \sin\varphi = 0,\ \chi \sin\varphi + 2\varepsilon \sin 2\varphi + \delta \cos\varphi = 0,\ \chi \cos\varphi + 4\varepsilon \cos 2\varphi - \delta \sin\varphi = 0. \quad (40)$$

It contains three expressions, which are consecutive derivatives of (36)in respect to parameter φ. As follows from the first and the third expressions of (40), $\cos 2\varphi = 0$, and $\chi \cos\varphi - \delta \sin\varphi = 0$. The first equation has two roots, $\varphi_1 = \pi/4$ and $\varphi_2 = 3\pi/4$. Hence, we get $\chi = \pm\delta$. Substituting this result in the second equation (40) we obtain

$$\chi = \mp\sqrt{2}\varepsilon. \qquad (41)$$

At $\varepsilon = 0{,}5$ this expression yields $\chi = \mp 0{,}707...$, in good correspondence with Fig. 15e, f.

The points with coordinates

$$\Delta = \frac{\chi^2}{2},\ \delta = \chi, \qquad (42)$$

and

$$\Delta = -\frac{\chi^2}{2},\ \delta = -\chi. \qquad (43)$$

in the plane (Δ, δ) correspond to the "dovetail" catastrophe. Thus, two "dovetail" structures appear simultaneously. They are located symmetrically on different bifurcation branches in the first and the third quarters of the plane (Fig. 15d). This is one of the manifestations of the symmetry of the system.

Figure 16 shows a chart of dynamical regimes for nonidentical, nonisochronous subsystems with inertial coupling. This figure has to be compared with Fig. 15f. (Note that in these two figures different scales are used.) In this chart, one can see an "inclined" structure of the period 1 regime predicted by the analysis of the phase dynamics. Herewith, typical "breaks" at its edges, associated with "dovetail" catastrophe, are clearly observable.

Figure 17 illustrates transformation of the synchronization region on the parameter plane (Δ, ε) as χ grows. These diagrams are plotted for $\delta = 0{,}5$ In this case the saddle-node bifurcation curves are defined by equations (36) and (37). Note that the last expression may be rewritten as

$$\varepsilon = \frac{\delta \sin\varphi - \chi \cos\varphi}{\cos 2\varphi}. \qquad (44)$$

The corresponding illustrations demonstrate that the nonisochronism leads to asymmetry of the synchronization region and to its displacement in accordance with a relation. From the figure one can see that a special situation corresponds to χ=δ. In this case, the formula (44) has an uncertainty at $\varphi = \pi/4$. In Fig. 17c we present a diagram for the "almost" bifurcation case. From Figs. 17c,d it follows that for χ>δ the "scenario" of the transformation of the synchronization region is reproduced in the reverse order, as χ grows.

In Fig. 18 a chart of dynamical regimes for nonidentical, nonisochronous subsystems with inertial coupling is shown on the plane (Δ, ε). One can see displacement of the synchronization region along the Δ axis, and its characteristic transformation. Unfortunately, the regions of phase bistability are not visualized by the used procedure of graphical presentation.

3.5. Inertial and dissipative couplings, nonidentity and nonisochronism

Now let us consider the most general case and account all the factors. Then, according to Eq. (12) we have

$$\Delta = 2\chi\delta + 2(\mu + \chi\varepsilon)\sin\varphi + \varepsilon^2 \sin 2\varphi + 2\varepsilon\delta\cos\varphi. \qquad (45)$$

Derivative of this relation with respect to φ leads to the expression

$$\delta = \frac{\varepsilon\cos 2\varphi + (\mu/\varepsilon + \chi)\cos\varphi}{\sin\varphi}. \qquad (46)$$

Combined with (45), it determines the synchronization region on the plane (Δ, δ). This region and its transformations are shown in Fig. 19. The diagrams are plotted at χ=0.75 and $\varepsilon = 0.5$; that is a case of "large" nonisochronism. The parameter value χ=0.75 corresponds to Fig. 15f. In Fig. 19 from panel (a) to (f) the parameter is decreased gradually from $\mu = 1{,}5$ to μ=-0.75.

The first panel (a) demonstrates the synchronization region in the form of an inclined "band". It has no singularities and tips. Bistability regions are absent.

Let us discuss the transformations of the synchronization region as μ decreases. First of all, we note that expression (46) is reduced to relation (38) via the parameter change $(\mu/\varepsilon + \chi) \to \chi$. Therefore, it is possible here to use the results of section 2.4. We conclude, that the transformation named "a horn to a horn" takes place at $\mu/\varepsilon + \chi = \pm\varepsilon$ or $\mu = \varepsilon(\pm\varepsilon - \chi)$. In turn, the "dovetail" catastrophes are observed at $\mu/\varepsilon + \chi = \pm\sqrt{2}\varepsilon$, or $\mu = \varepsilon(\pm\sqrt{2}\varepsilon - \chi)$

At fixed χ and ε, the following transformations take place as μ decreases (Fig. 19). At $\mu_1 = \varepsilon(\sqrt{2}\varepsilon - \chi)$ the "dovetail" catastrophe occurs. As a result, two small regions of bistability are formed (Fig. 19b). Then "a horn to a horn" transformation takes place at $\mu_2 = \varepsilon(\varepsilon - \chi)$, and the regions of bistability merge (Fig. 19c). At further decrease of μ, a second "a horn to a horn" transformations occurs at $\mu_3 = -\varepsilon(\varepsilon + \chi)$ and the "dovetail" catastrophe takes place at $\mu_4 = -\varepsilon(\sqrt{2}\varepsilon + \chi)$ (Fig. 19d, e). As a result, we arrive at a configuration of Fig. 19f, which is similar to the initial one (Fig. 19a). Note that so far we considered the case $\mu < 0$ (i.e. the case of active coupling). However the first two transformations (Figs. 19a-c) as well can be observed also in the case of dissipative coupling provided the inequality $\chi < \varepsilon$ holds.

In the parameter plane (Δ, ε), similar transformations are observed. They can be also easily found analytically from (46). Therefore, we do not present in details the corresponding results.

Figure 20 shows charts of dynamical regimes for nonidentical, nonisochronous subsystems with dissipative and inertial coupling. Here panel (a) corresponds to dissipative coupling $(\mu > 0)$ and panel (b) to active coupling $(\mu < 0)$.The diagrams can be regarded as modifications of Fig. 16. It is the case when

all four physical factors controlling the behavior of the coupled van der Pol systems are relevant. One can see that the dissipative coupling leads to broadening of the main synchronization region at $\mu > 0$ (compare Fig. 20a and Fig. 16). At $\mu < 0$ this widening is not so pronounced, but a noticeable widening of the synchronization regions of higher order takes place (Fig. 20b).

Conclusion

In the present work we discussed synchronization phenomena in a system of non-identical, non-isochronous van der Pol – Duffing oscillators with dissipative and inertial coupling. The general Adler equation describing the phase dynamics was derived for this system. It was shown that all factors except the dissipative coupling demand to take into account effects of the second order for correct description of the phase dynamics. For example, nonidentity or nonisochronism are found to affect the synchronization picture only in the presence of inertial coupling. Hence, the combination of the effects is relevant. It was shown that the phase equation possesses a certain set of symmetries. The bifurcation portrait of the system on the parameter plane was discussed within the framework of the phase equation. In this case, the conditions of the transformations of the picture under parameter variations may be deduced analytically.

The structure of the parameters space of coupled van der Pol – Duffing oscillators was studied with application of the method of charts of dynamical regimes in computations from initial differential equations for non-identical, non-isochronous subsystems with dissipative and inertial coupling. Beside the features predicted from analysis of the phase equations (form of the main synchronization region, bistability, etc.), some other essential moments were found and discussed (organization of the higher order synchronization tongues, chaotic regions, etc.) that are not be described in the frame of the phase equation approach. In general, the model associated with the initial differential equations is characterized by a large number of parameters. Therefore, its complete numerical analysis is far more difficult in comparison with a study of the dynamics with the phase equation. The computer simulation also confirms equivalence, up to certain degree, for some types of behaviors associated with symmetries of the phase equation.

Acknowledgements

We thank S.P. Kuznetsov and I.R. Sataev for help and discussions. This research was supported, in part, by the grant 2.1.1/1738 of Ministry of Education and Science of Russian Federation in a frame of program of Development of Scientific Potential of Higher Education. A.P.K. and L.V.T. acknowledge a partial support from the RFBR grant No 09-02-00426. N.V.S. acknowledges a partial support from the RFBR grant No 09-02-00707.

References

1. *Pikovsky A., Rosenblum M., Kurths J.* Synchronization. A universal concept in nonlinear sciences. Cambridge, 2001, 411p.
2. *Aronson D.G., Ermentrout G.B., Kopell N.* Amplitude Response of Coupled Oscillators. // Physica D, 1990, Vol. 41, p. 403.
3. *Rand R., Holmes.* Bifurcation of Periodic Motions in Two Weakly Coupled van der Pol Oscillators. // Int. J. Non-Linear Mechanics, 1982, Vol. 17, p. 143-152.
4. *Storti D.W., Rand R.H.* Dynamics of Two Strongly Coupled van der Pol Oscillators. // Int. J. Non-Linear Mechanics, 1980, Vol. 15, p. 387-399.
5. *Chakraborty T., Rand R.H.* The Transition From Phase Locking to Drift in a System of Two Weakly Coupled van der Pol Oscillators. // Int. J. Non-Linear Mechanics, 1988, Vol. 23, No. 5/6, p. 369-376.
6. *Poliashenko M., McKay S.R., Smith C.W.* Chaos and Nonisochronism in Weakly Coupled Nonlinear Oscillators. // Phys. Rev. A., 1991, Vol. 44, p. 3452.
7. *Poliashenko M., McKay S.R., Smith C.W.* Hysteresis of Synchronous – Asynchronous Regimes in a System of Two Coupled Oscillators. // Phys. Rev. A., 1991, Vol. 43, p. 5638.
8. *Pastor I., Perez-Garcia V.M., Encinas-Sanz F., Guerra J.M.* Ordered and Chaotic Behavior of Two Coupled van der Pol Oscillators. // Phys. Rev. E., 1993, Vol. 48, p. 171.
9. *Camacho E., Rand R.H., Howland H.* Dynamics of Two van der Pol Oscillators Coupled via a Bath. // Int. J. of Solids and Structures, 2004, Vol. 41, p. 2133-2143.

10. *A. K. Kozlov; M. M. Sushchik; Ya. I. Molkov; A. S. Kuznetsov*. Bistable phase synchronization and chaos in a system of coupled van der Pol – Duffing oscillators. // International Journal of Bifurcation and Chaos, 1999, No. 12, p. 2271-2277.
11. *Kuznetsov A.P., Paksyutov V.I.* About dynamics of the two dissipative-coupled van der Pol – Duffing oscillators. // Applied Nonlinear Dynamics, 2003, Vol. 11, No. 6, p. 48 - 64.
12. *Kuznetsov A.P., Paksyutov V.I.* Feature of the parameter space structure of two nonidentical coupled van der Pol – Duffing oscillators. // Applied Nonlinear Dynamics, 2005, Vol. 13, No. 4, p. 3-19.
13. *Ivanchenko M.V., Osipov G.V., Shalfeev V.D., Kurths J.* Synchronization of two non-scalar-coupled limit-cycle oscillators. // Physica D, 2004, Vol. 189/1-2, p. 8-30.
14. *Cohen D.S., Neu J.C.* Interacting oscillatory chemical reactors. Ann. N.Y. Acad. Sci. 316, Bifurcation Theory and Applications in the Scientific Disciplines (ed. O. Gurel and O.E. Rössler), 1979, p. 332-337.
15. *Neu J.C.* Coupled chemical oscillators // SIAM J. appl. Math, 1979, Vol. 37(2), p.307-315.
16. *Pavlidis T.* Biological oscillators: The Mathematical Analysis. Academic press, 1973.
17. *Mettin R., Parlitz U., Lauterborn W.* Bifurcation Structure of the Driven van der Pol Oscillator. // International Journal of Bifurcation and Chaos. 1993, Vol. 3. No. 6.
18. *Guckenheimer J., Holmes Ph.* Nonlinear Oscillations, Dynamical Systems and Bifercations of Vector Fields. Springer-Velag New York Inc, 1983.
19. *A.P.Kuznetsov, S.P.Kuznetsov, I.R.Sataev*. A variety of period-doubling universality classes in multi-parameter analysis of transition to chaos. // Physica D, 1997, Vol. 109, p. 91-112.
20. *A. P. Kuznetsov, E. Mosekilde and L.V. Turukina* Synchronization in systems with bimodal dynamics. // Physica A121, 2006, No. 2, p. 280-292.
21. *Carcasses J., Mira C., Bosch M., Simo C. & Tatjer J.C.* «Crossroad area - spring area» transition (I) Parameter plane representation. // Int. J. Bif. & Chaos, 1991, Vol. 1, No. 1, p.183-196.
22. *Carcasses J., Mira C., Bosch M., Simo C. & Tatjer J.C.* «Crossroad area - spring area transition» (II) foliated parametric representation. // Int. J. Bif. & Chaos, 1991, Vol. 1, No. 2, p.339-348.
23. *Poston T., Stewart I.* Catastrophe theory and its applications. London, 1978
24. *Arnold V.I.* Catastrophe theory. Springer, Berlin, 1984.
25. *A. P. Kuznetsov, V. I. Paksyutov and Yu. P. Roman.* Features of the synchronization of coupled van der Pol oscillators with nonidentical control parameters. // Technical Physics Letters, 2007, No. 8, p. 636-638.
26. *Kuznetsov A.P., Yu.P. Roman*. Synchronization of coupled anizochronous oscillators. // arXiv:0806.1402v1.
27. *Kuznetsov A.P., Kuznetsov S.P.* Critical dynamics of coupled map lattices at the onset of chaos (review). // Izv. Vuz. «Radiofizika», 1991, Vol. 34, No. 10-12, p. 1079-1115.

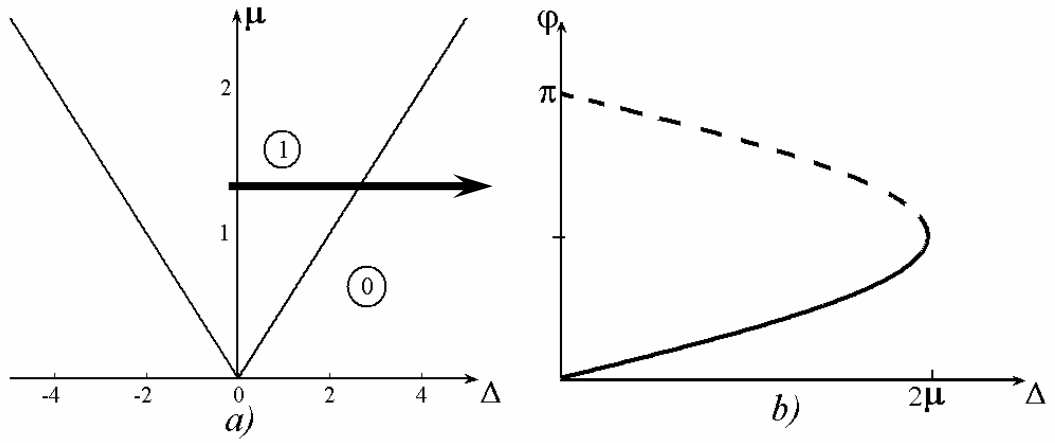

Fig. 1. Synchronization region on the parameter plane the (μ, Δ) for a system with dissipative coupling (a) and the bifurcation diagram (b) drawn along the route on the parameter plane indicated by arrow. Bifurcation diagram plotted along line represented by arrow in the fig. a.

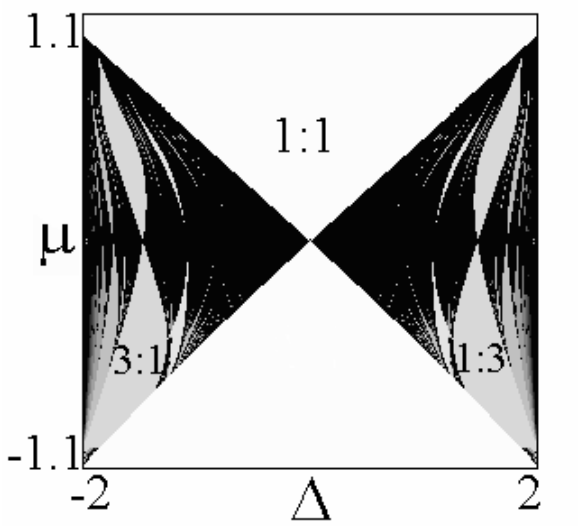

Fig. 2. Chart of dynamical regimes obtained in computations for a set of differential equations of a system with dissipative coupling in the parameter plane (Δ, μ) at $\lambda_1 = \lambda_2 = 1$ and $\beta = 0$.

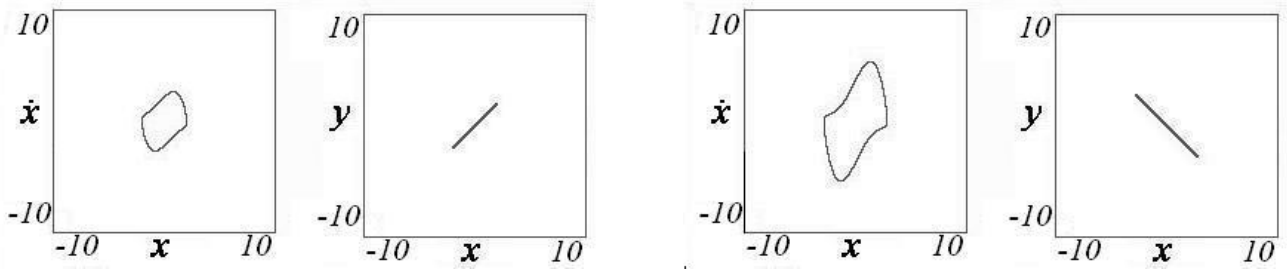

а) **б)**

Fig. 3. Portraits of attractors in projection on the plane $(x, \dot{x})$ and Lissajous figures on the plane (x, y) for systems with dissipative (a) and active (b) couplings at $\lambda_1 = \lambda_2 = 1$, $\Delta = 0.01$, and $\mu = 0.5$.

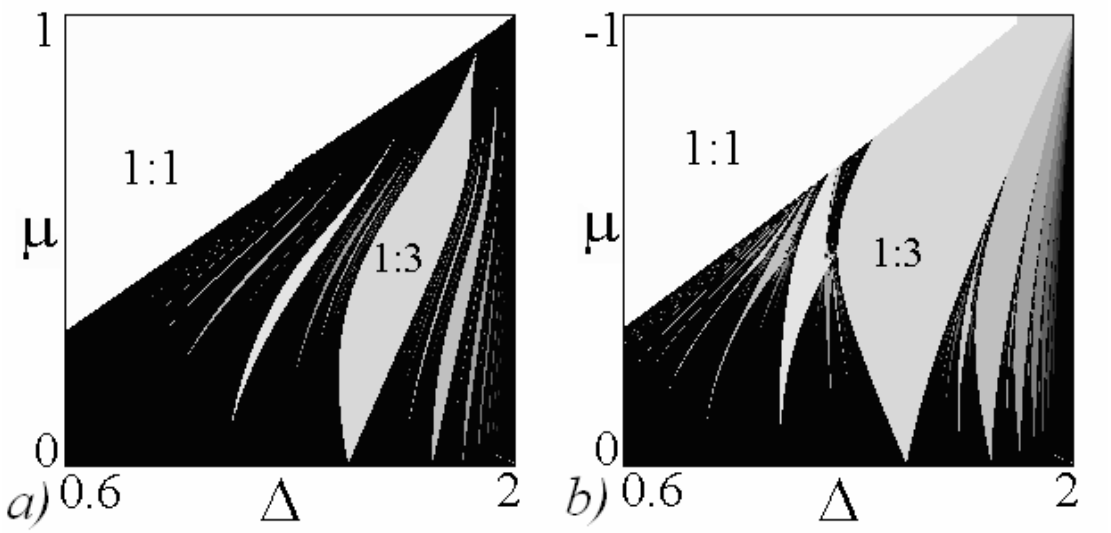

Fig. 4. Fragment of the diagram of Fig. 2 for systems with dissipative (a) and active (b) coupling at $\lambda_1 = \lambda_2 = 1$ and $\beta = 0$.

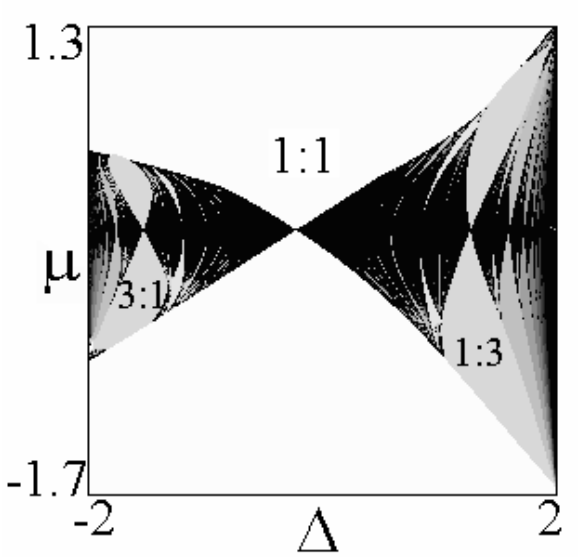

Fig. 5. Chart of dynamical regimes of the system of non-identical oscillators with dissipative coupling in the parameter plane (Δ, μ) for $\lambda_1 = 2$, $\lambda_2 = 1$ and $\beta = 0$.

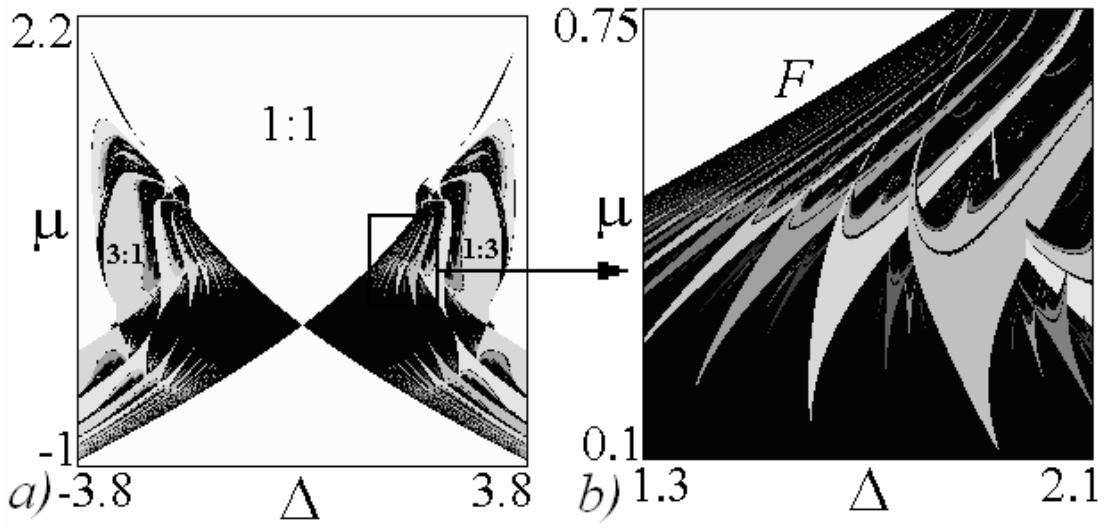

Fig. 6. Chart of dynamical regimes (a) and its fragment (b) for a system of nonisochronous oscillators with dissipative coupling in the parameter plane (Δ, μ) for $\lambda_1 = \lambda_2 = 1.0$ and $\beta_1 = \beta_2 = 0{,}5$. The saddle-node bifurcation is marked with *F*.

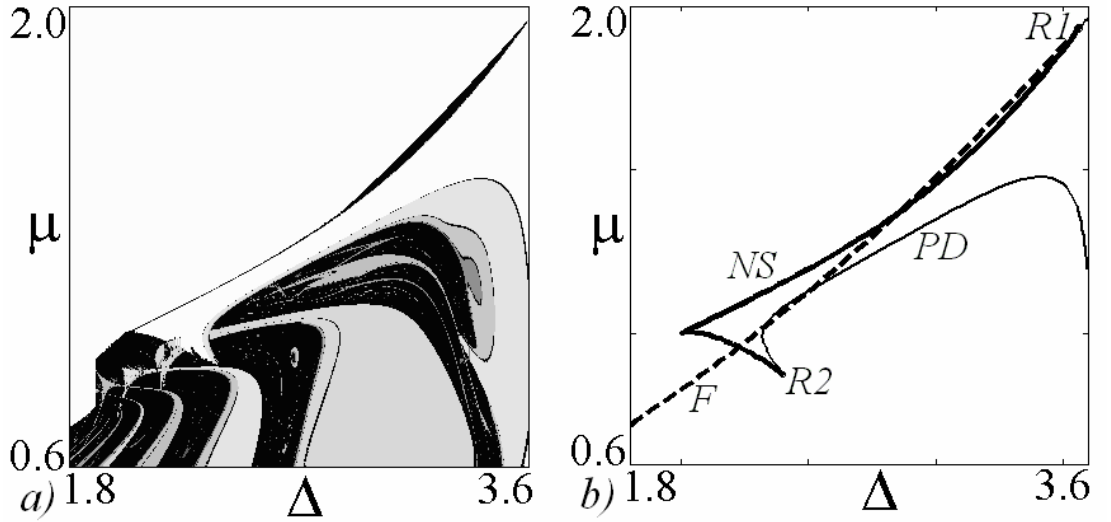

Fig. 7. Fragment of the chart of dynamical regimes from Fig.6 (a). Curves and points of bifurcations for system on the same parameter plane (b). The Neimark-Saker bifurcation is indicated with *NS*, the saddle-node bifurcation with *F*, and the period-doubling bifurcation with *PD*. *R*1 designates a point of resonance 1:1, and *R*2 corresponds to the resonance 1:2.

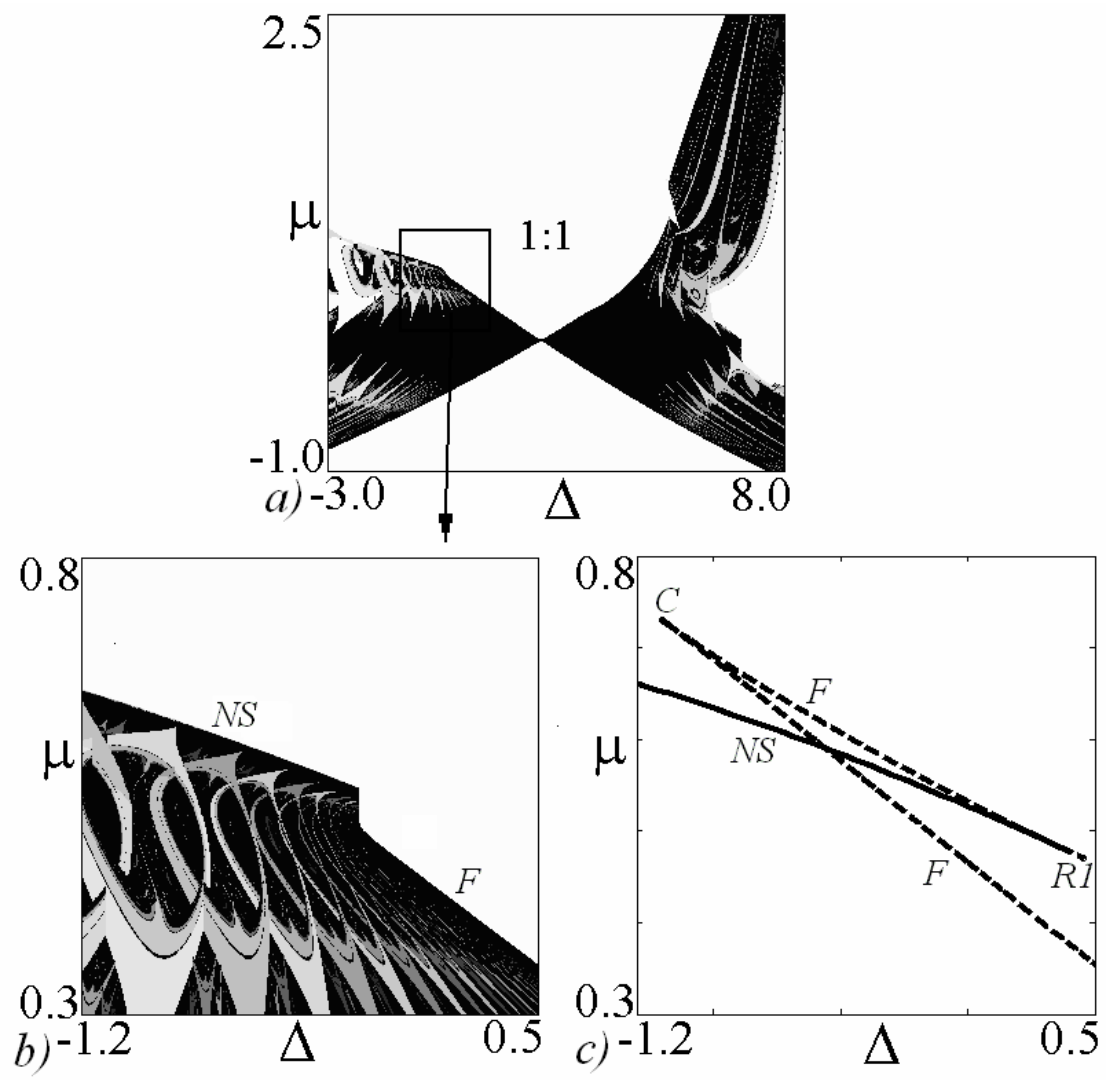

Fig. 8. Chart of dynamical regimes for non-identical, nonisochronous oscillators with dissipative coupling in the parameter plane (Δ, μ) at $\lambda_1 = 2$, $\lambda_2 = 1$, δ=0,5, $\beta_1 = \beta_2 = 1$ (a) and its fragment (b). Curves and points of bifurcations on the parameter plane (c). *NS* marks the Neimark-Saker bifurcation and *F* indicates the saddle-node bifurcation. *R*1 designates the point of resonance 1:1, *C* is the cusp point.

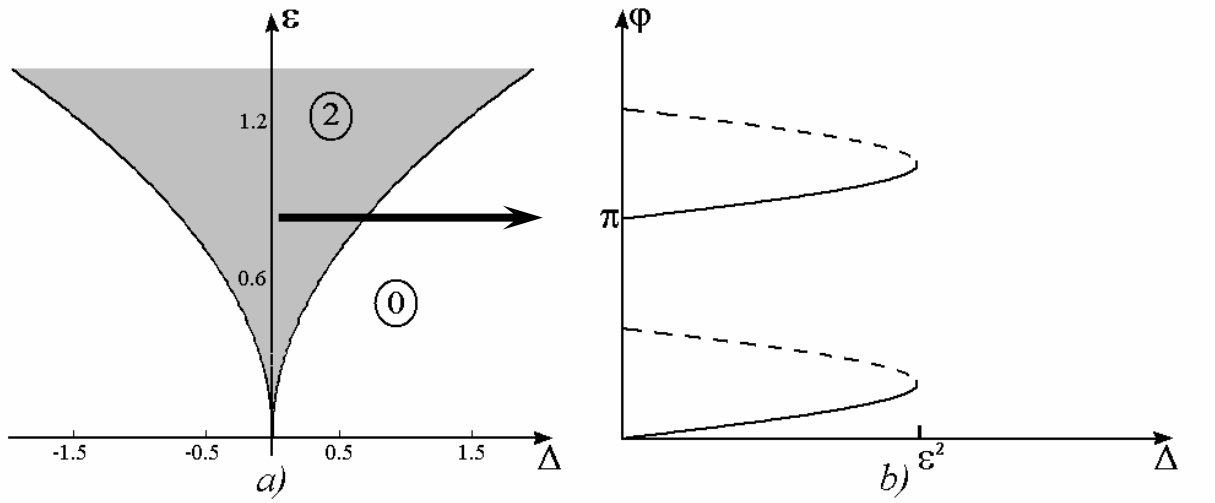

Fig. 9. Synchronization region of the system with inertial coupling in the parameter plane (ε, Δ) (a) and the bifurcation diagram on the route shown by the arrow (b).

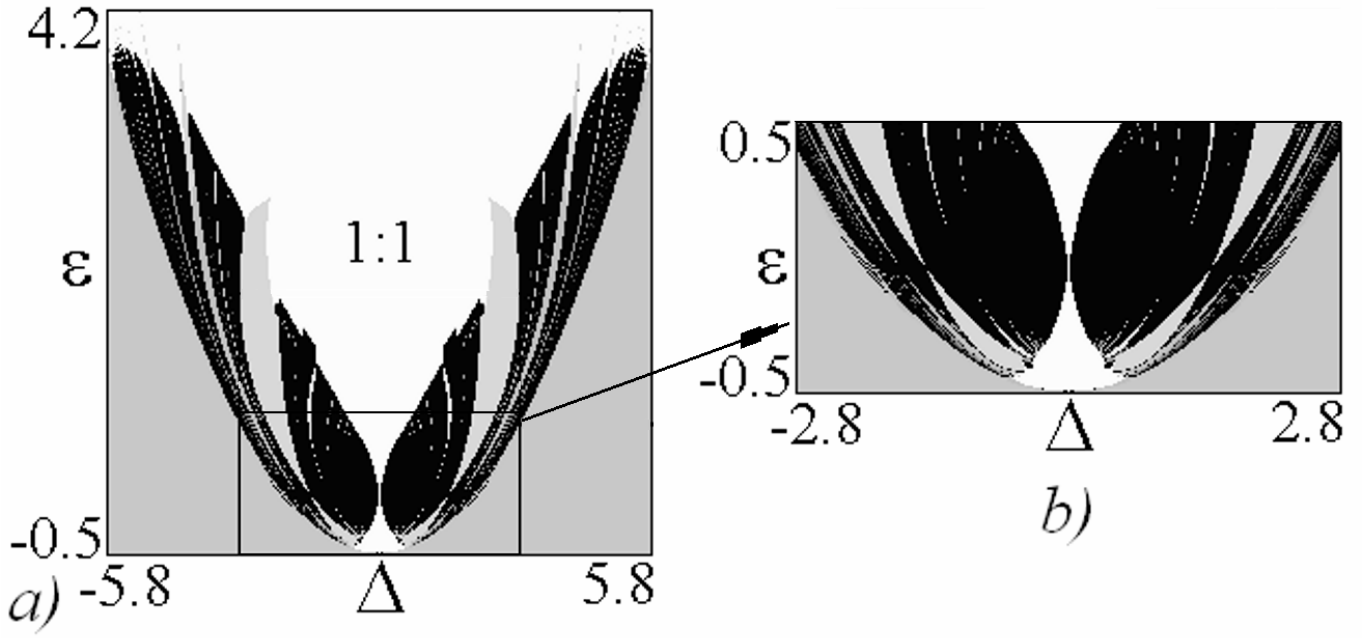

Fig. 10. a) Chart of dynamical regimes (a) and its fragment (b) for the system with inertial coupling in the parameter plane (ε, Δ) at $\lambda_1 = \lambda_2 = 1$ and $\beta = 0$. The uniformly colored gray areas at the left and the right edges of the picture correspond to divergence of the orbits to infinity.

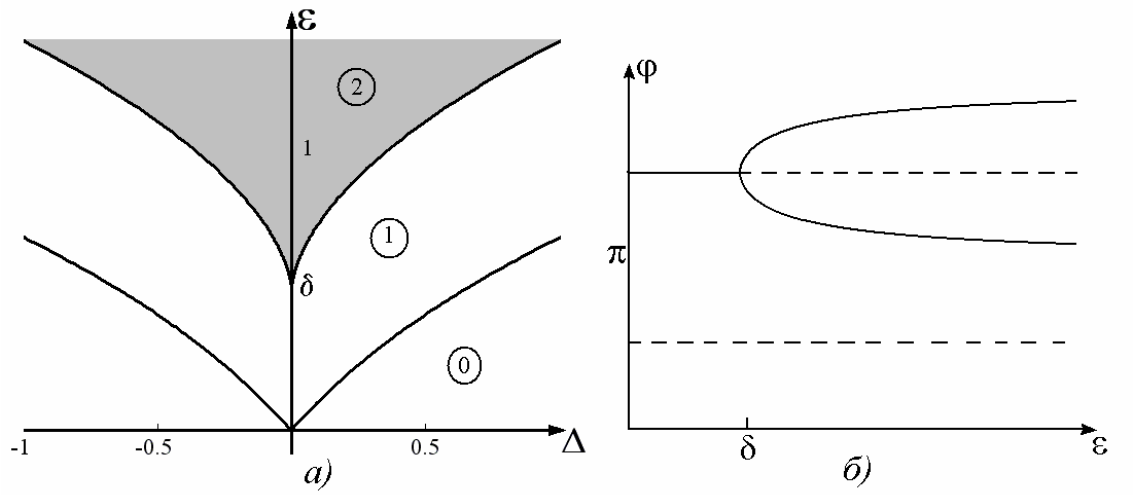

Fig. 11. Synchronization region of non-identical systems with inertial coupling in the parameter plane (ε, Δ) for δ=0,5 (a) and the bifurcation diagram drawn for a route along the line $\Delta = 0$ (b).

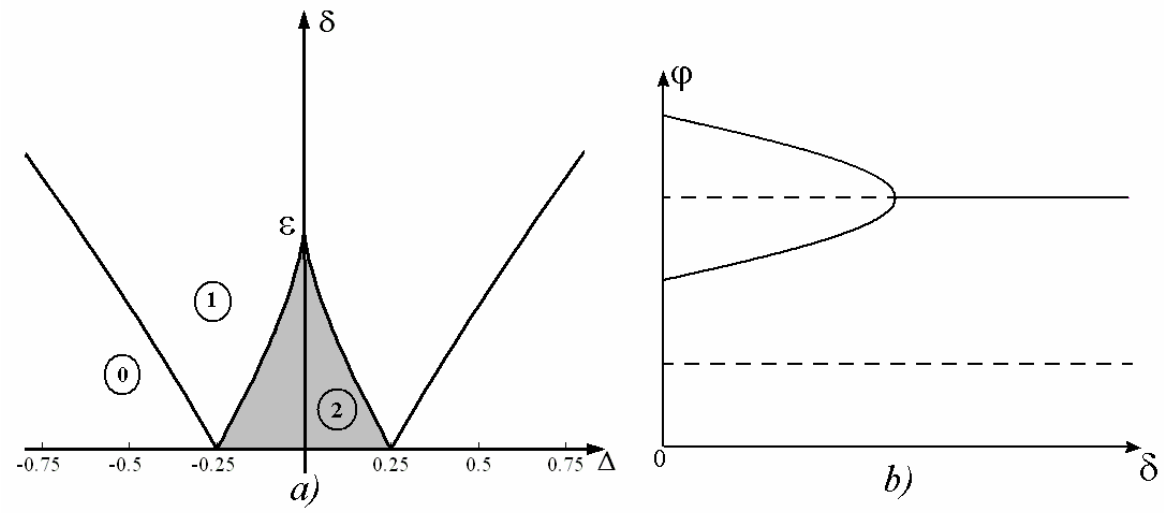

Fig. 12. Synchronization region of the system of non-identical oscillators with inertial coupling in the parameter plane (δ, Δ) for ε=0.5 (a) and the diagram drawn for a route along the line $\Delta = 0$ (b).

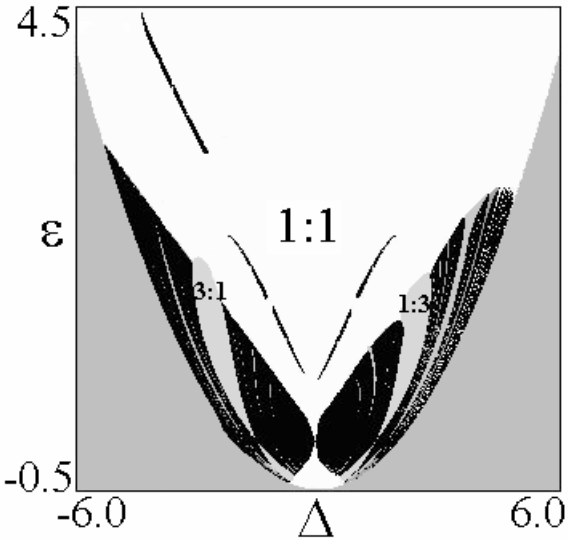

Fig. 13. Chart of dynamical regimes of the system of non-identical oscillators with inertial coupling in the parameter plane (ε, Δ) for δ=0,5 (λ_1=2 и λ_2=1).

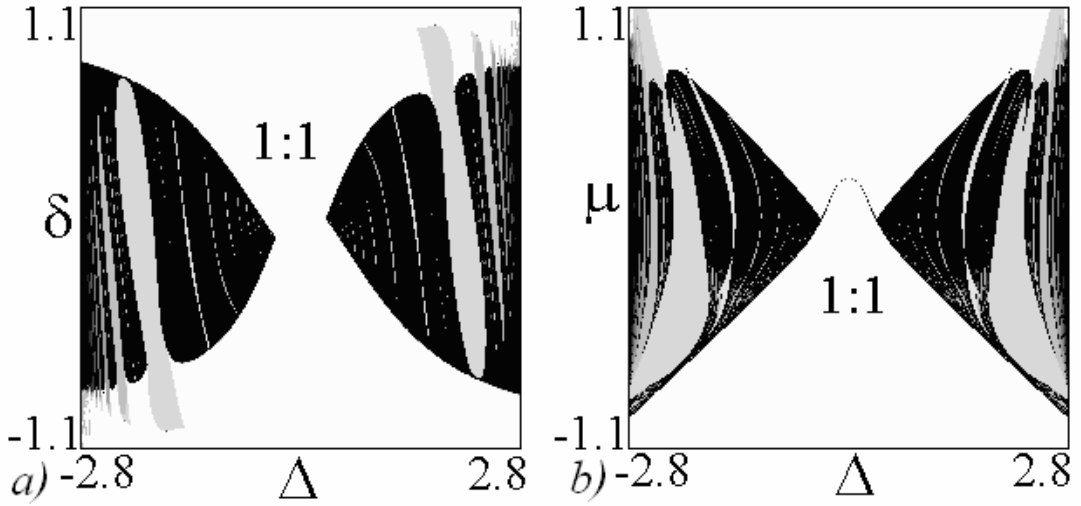

Fig. 14. A chart of dynamical regimes for non-identical oscillators with inertial coupling (a) and for oscillators with combined inertial and dissipative coupling (b). The charts are plotted for ε=0,5.

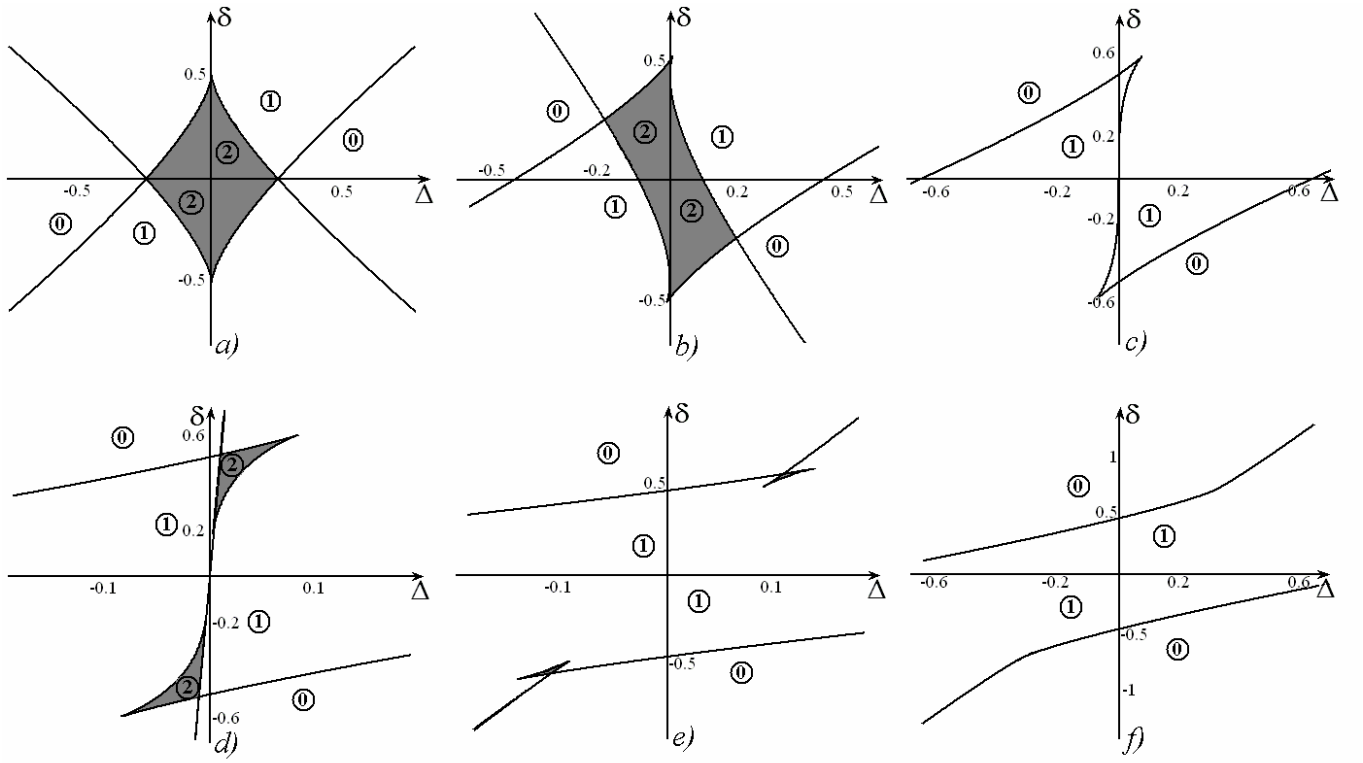

Fig. 15. A set of diagrams illustrating transformation of the bifurcation lines in the parameter plane (Δ, δ) for non-identical, nonisochronous systems with inertial coupling under variation of parameter χ at $\varepsilon = 0.5$. Here χ=0 (a); χ=0,25 (b); χ=0,5 (c); χ=0,51 (d); χ=0,6 (e); χ=0,75 (f).

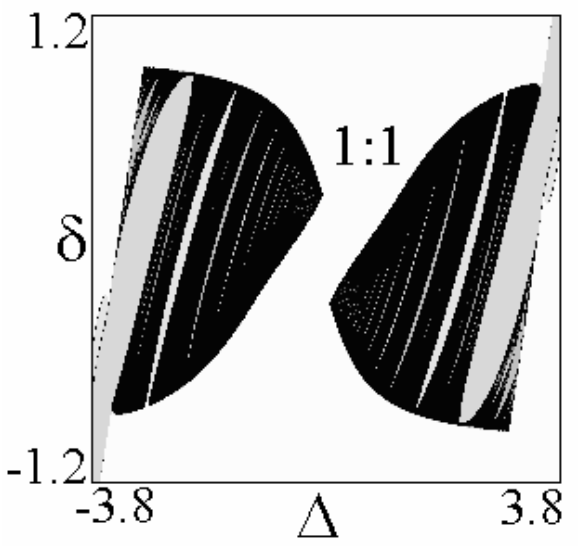

Fig. 16. Chart of dynamical regimes for non-identical, nonisochronous oscillators with inertial coupling in the parameter plane (δ, Δ) for ε=0, χ=0.75, β=0.25.

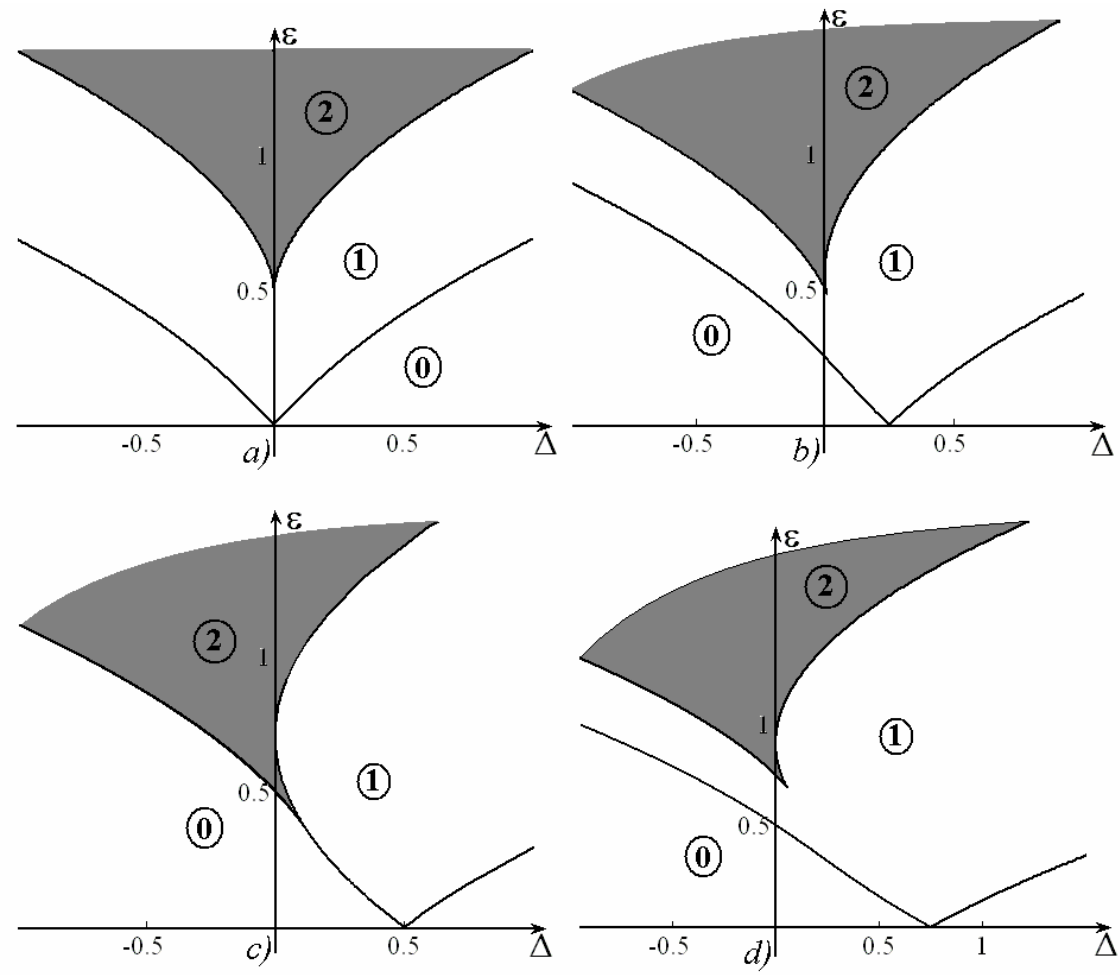

Fig. 17. A set of diagrams illustrating transformation of the bifurcation lines in the parameter plane (Δ, ε) for non-identical, nonisochronous systems with inertial coupling under variation of parameter χ at $\delta = 0.5$. Here χ=0 (a); χ=0,25 (b); χ=0,4999 (c); χ=0,75 (d).

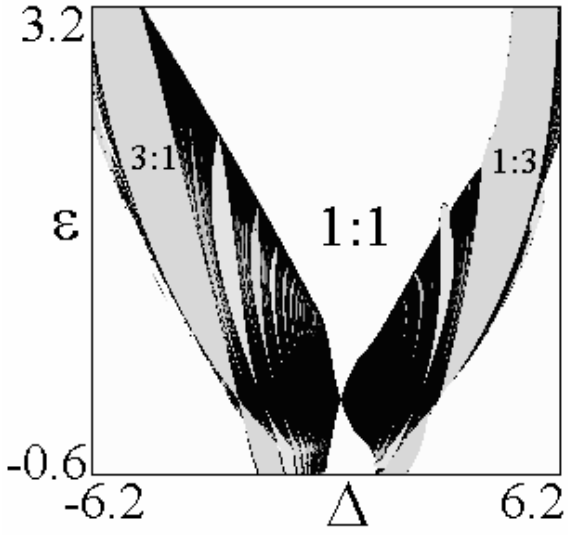

Fig. 18. Chart of dynamical regimes of non-identical, nonisochronous oscillators with inertial coupling in the parameter plane (ε, Δ) for δ=0,5 (λ_1=2 и λ_2=1) and χ=0,75 (β=0,25).

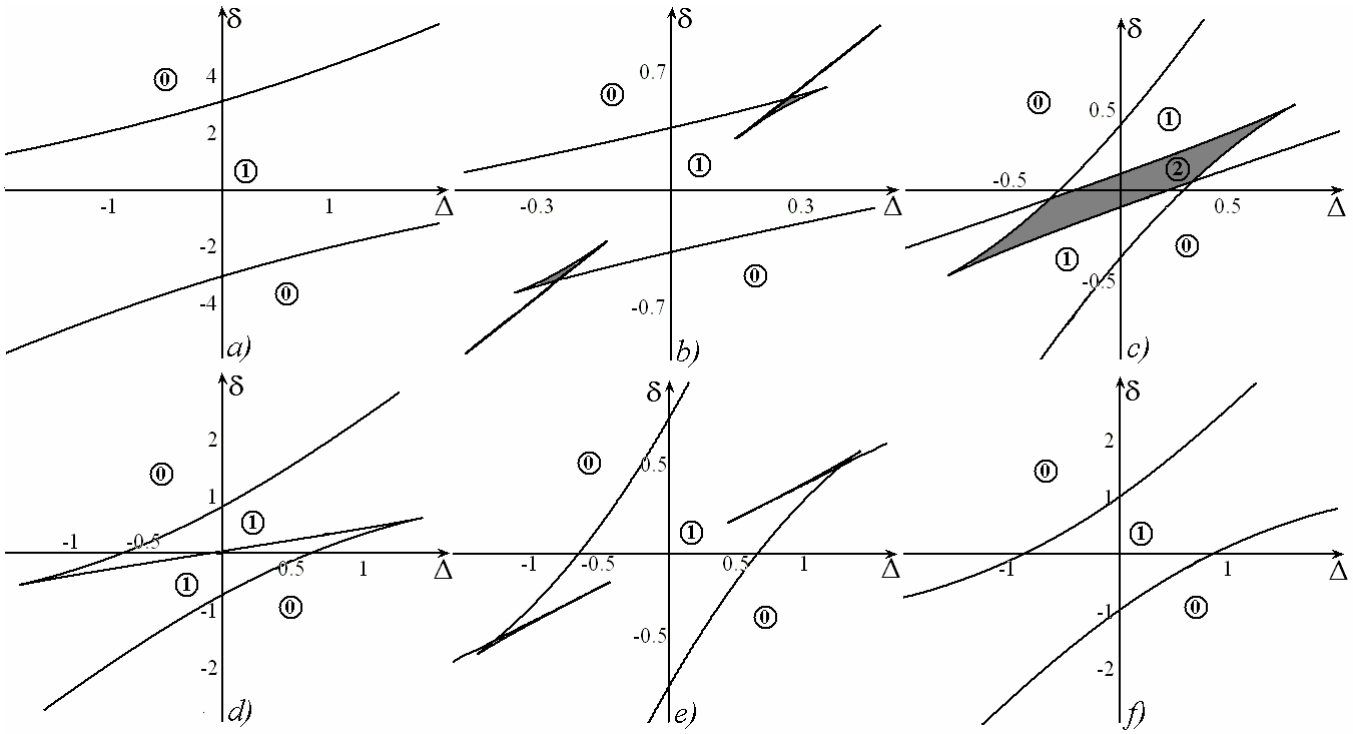

Fig. 19. A set of diagrams illustrating transformation of the bifurcation lines in the parameter plane (Δ, δ) for non-identical, nonisochronous systems with inertial and dissipative coupling under decrease of parameter μ: a) μ=1,5; b) μ=-0,11; c) μ=-0,4; d) μ=-0,625; e) μ=-0,63; f) μ=-0,75. at $\delta = 0.5$. Fig. 15f shows the case of μ = 0. The diagrams are plotted for $\varepsilon = 0.5$ and χ=0.75.

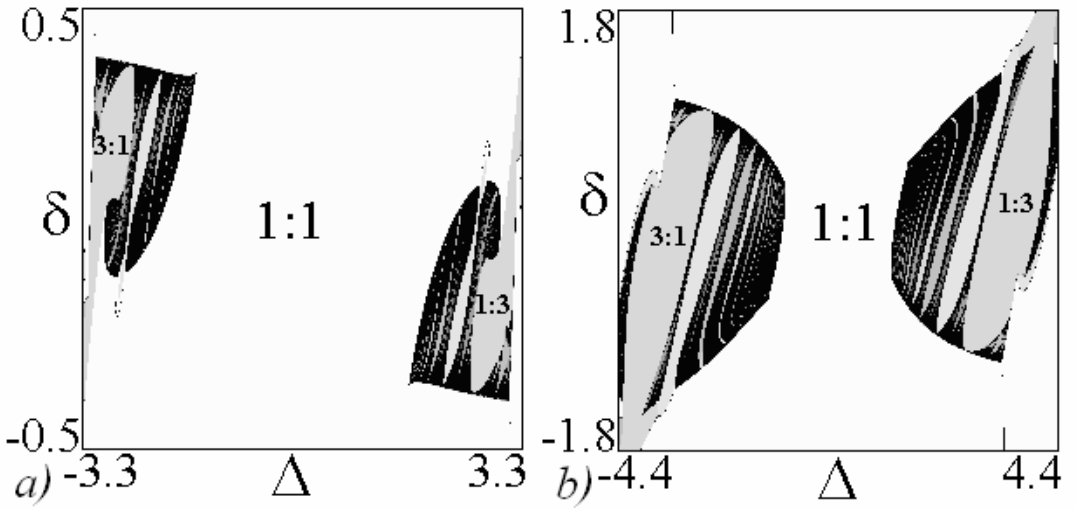

Fig. 20. Charts of dynamical regimes for non-identical, nonisochronous oscillators with inertial and dissipative coupling in the parameter plane (Δ, δ) for χ=0.75, ε=0.5, μ=0.6 (a) and μ=-0.4 (b).